Cr/Sc multilayers for the soft-x-ray range

Franz Schäfers, Hans-Christoph Mertins, Frank Schmolla, Ingo Packe,
Nikolay N. Salashchenko, and Eugeny A. Shamov

We have systematically investigated ultrathin Cr/Sc multilayers (nanolayers), using tunable soft-x-ray synchrotron radiation. The multilayers were optimized for use either in normal incidence or at 45° at photon energies around the 2*p*-absorption edges of Sc (399 eV) and Cr (574 eV), respectively. They were sputter deposited on Si wafers or on thin Si_3N_4-membrane support structures for use in reflection and in transmission, respectively, as polarizing and phase-retarding elements in a polarimeter. The performance theoretically expected with respect to reflection/transmission and energy resolution has been confirmed experimentally: A value of 7% for the normal-incidence peak reflectance at 395 eV was measured as well as a pronounced minimum in transmission for certain incidence angles and energies below the respective absorption edges, indicating significant phase-shifting effects. © 1998 Optical Society of America

OCIS codes: 230.4170, 350.5610, 120.5700, 120.7000.

1. Introduction

Multilayers with periods in the atomic range of 1–2 nm (nanolayers) are currently of great interest. This interest is related to their widespread use, e.g., as radiation-stable dispersive optical elements[1,2] and polarizers for synchrotron radiation,[3–6] as dispersive elements for x-ray diagnostics of high-temperature plasmas,[7,8] as normal-incidence reflectors for (soft-) x-ray microscopy in the water window (284–530 eV),[9] and for applications in x-ray astronomy.[10]

All these applications require high-radiation and -thermal stability, high spectral selectivity, and, in particular, high reflectance. A normal-incidence reflectance of 5% is considered to be sufficient for many applications, e.g., for double-mirror systems in telescopes and microscopes. For photon energies up to the C 1*s* edge (284 eV), mirrors, including spherical ones, on the basis of Fe/C and Cr/C with reflectances between 6% and 13% are available.[11,12] However, for photon energies greater than 284 eV the reflectance has not until recently exceeded 3%.[13]

It has recently been shown that specially optimized multilayer systems working both in reflection and in transmission [Mo/Si, 95 eV (Ref. 3) and Cr/C, 265 eV (Ref. 4)] can be used effectively for a complete polarization analysis of soft-x-ray radiation distinguishing among linear, circular, and unpolarized components, i.e., all four Stokes parameters. At 95 eV this system is also routinely used for a complete conversion of linearly into circularly polarized radiation, since the Mo/Si transmission multilayer operates as a perfect quarter-wave plate.[6] For higher photon energies above the C 1*s* edge, phase-retarding transmission multilayers have been proposed,[5] but so far not realized.

The layer thickness scales with the wavelength. Thus with increasing energy the performance of a multilayer is increasingly influenced by the interface roughness σ, according to the Debye–Waller-type term in the reflectance: $R = R_0 \exp[-(2\pi m\sigma/d)^2]$, where R_0 is the reflectance of an ideal structure with $\sigma = 0$ nm and m is the reflection order. Thus, with decreasing period d the reflectance tends to be dominated by the Debye–Waller factor and the ratio σ/d rather than by the optimum choice of material pairs in terms of their x-ray optical constants.

Consequently, the optimum material pairs will be those that yield structures with minimum interfacial roughness. For example, for pairs such as W/Sb, W/Sc,[12,14] and W/B_4C,[15] no increase in roughness with decreasing period has been reported. For such a widely used pair as W/Si, however, no high-reflectance structures with $d < 1.6$ nm have been

F. Schäfers, H.-C. Mertins, F. Schmolla, and I. Packe are with BESSY mbH, Lentzeallee 100, D-14195 Berlin, Germany. N. N. Salashchenko and E. A. Shamov are with the Institute for Physics of Microstructures, Russian Academy of Sciences, 603600 Nizhny Novgorod GSP 105, Russia.

Received 27 June 1997; revised manuscript received 8 October 1997.

0003-6935/98/00719-10$10.00/0

reported so far. The interest in multilayers containing Sc is called forth by the high reflection in the range of the anomalous dispersion at the Sc 2*p*-absorption edge at 399 eV. In particular for W/Sc, Cr/Sc, and Fe/Sc a high reflectance was realized.[13,16,17] But efforts to produce high-reflectance structures of Cr/Sc and Fe/Sc with $d < 2$ nm have failed so far.

In this paper we present a systematic experimental investigation on a variety of Cr/Sc multilayers with period thicknesses between 1.5 and 3.1 nm using tunable synchrotron radiation. The period and the thickness ratio of the multilayers were tailored to their specific application with special emphasis on their use at the absorption edges of Cr (574 eV) and Sc (399 eV), respectively. They were optimized for the following synchrotron radiation applications:

(1) High-reflectance normal-incidence mirrors for the water window.

(2) Polarimetry in the soft-x-ray range (detectors for polarized light).

(a) Reflection multilayers to analyze linearly polarized light (45°, Rabinovitch detectors).

(b) Transmission multilayers to convert circularly into linearly polarized light (phase retarders, $\lambda/4$ plates).

Application (2) is part of a project of extending the working range of multilayer polarimeters to higher photon energies above the C 1*s* edge.[18]

2. Theory

A. Choice of Materials

With increasing photon energy the refractive index of the absorber and the spacer materials of a multilayer approaches 1 and thus the reflectances at the interfaces decrease. Nevertheless, the reflectance is drastically enhanced right below the absorption edges of the involved materials because of the low imaginary part and the high real part of the Fresnel reflection coefficient in these regions.

In Fig. 1 the maximum achievable normal-incidence reflectance was calculated on the basis of the Henke tables[19] for various Fe, W, Cr multilayers with C, Sb, or Sc as spacers. For calculations using the BESSY-REFLEC program[20] is used, 200 periods, equal thicknesses of absorber and spacer materials ($\gamma = 0.5$) and ideal structures with no roughness were assumed. The *d* spacing of the multilayer was varied with photon wavelength λ according to $d = \lambda/2$. The C, Sc, Sb, and Cr resonances show up with ideal reflectances as high as 55%. Fe as an absorber is superior to W and Cr. The performance of other material combinations such as W/Ti, Ni/Ti, and Ni/V for the water window have been investigated in Ref. 21.

In this investigation we focused exclusively on Cr as an absorber and Sc as a spacer material due to promising earlier experimental data.[16,17] Because of the enhancement of the multilayer performance

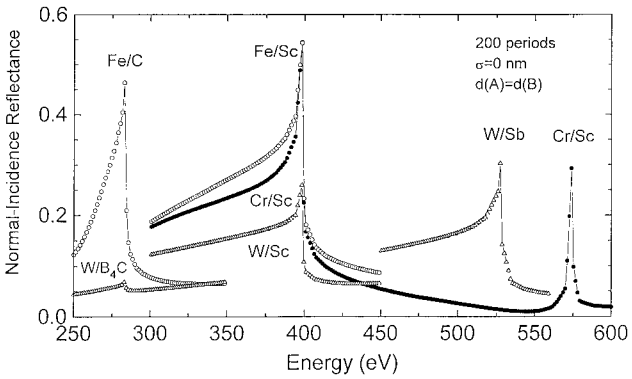

Fig. 1. Survey of theoretical multilayer performance in the water window region. The maximum normal-incidence reflectance for ideal multilayers, assuming no roughness, is plotted. The *d* spacing is varied with the photon wavelength according to $\lambda = 2d$. In the calculation 200 periods and equal thicknesses were assumed for all multilayers. The best performance is obtained at and below the absorption edges of the respective spacer materials.

near absorption edges, we concentrated the investigation on the Sc and the Cr 2*p* edges at 399 and 574 eV, respectively. According to the procedure described in Ref. 22 the choice of an optimum material combination for a certain photon energy is made on the basis of a complex plot of the reflection coefficients. This is shown in Fig. 2 as an example for the Sc 2*p* edge, where the imaginary part of the normal-incidence reflection coefficient is plotted against its real part. As seen in Fig. 1, the transition metal, (Fe, Ni, Co) Sc, combination is superior to a noble metal, (W, Ir, Os, Pt) Sc, combination because of the higher absorption of the latter. According to the selection criterion of Fig. 2, Cr/Sc seems inappropriate because of poor contrast. However, this criterion does not take roughness into account, which, according to previous experimental data,[16,17] favors this material combination.

B. Theoretical Analysis and Processing of X-Ray Diffraction Spectra

The analysis of small-angle x-ray diffraction spectra is a standard method for determining the parameters of multilayers.[23] These parameters, such as the interfacial roughness dispersion σ^2, the thickness of films d_1, d_2, and others, are determined by fitting the angular dependence of the measured reflectance with CuK_α radiation in the region of total external reflection and of a few Bragg maxima. For the analysis of superthin ($\leq$1 nm) multilayers, however, the use of this procedure is quite problematic. In such a case typically only the first-order Bragg maximum is observed owing to the rapid decrease in the higher-order reflectance (Section 1) with the decrease in the period. Here we present an alternative procedure that was applied to the Cr/Sc samples of this article. This procedure is based on the analysis of the angular dependence of the reflectance at several different

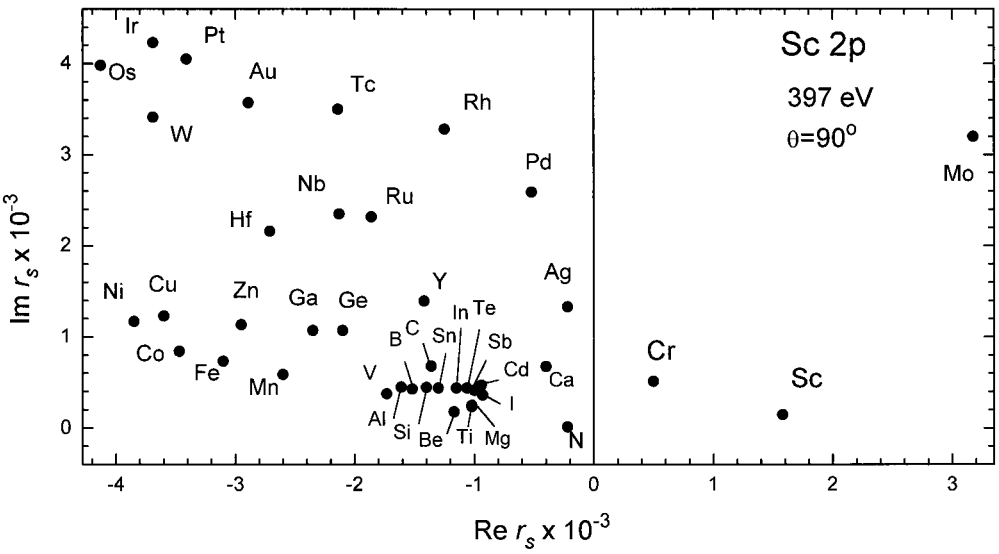

Fig. 2. Plot of imaginary versus real part of the normal-incidence reflection coefficients for a variety of materials at a photon energy of 397 eV (Sc 2*p* edge) according to Ref. 22.

wavelengths. In the kinematic approach the reflectance has the form[23]

$$R(\theta) = [k_0^2 \sin \pi\gamma/(\pi q)]^2 |\varepsilon_1 - \varepsilon_2|^2 \exp(-q^2\sigma^2) \times \left| \int_0^L \exp\{i[kz + \Phi(z)]\} \mathrm{d}z \right|^2, \quad (1)$$

with

$$k = [2k_0^2/q](\sin^2 \theta_B - \sin^2 \theta),$$

$$\Phi(z) = (q/d) \int_0^Z \xi(z') \mathrm{d}z,$$

where θ is the grazing angle of incidence of the radiation, $k_0 = 2\pi/\lambda$ is the wave number in vacuum, $d = 2\pi/q$ is the period, $\xi(z')$ is the local thickness deviation, $\gamma = d_1/d$ is the thickness ratio, L is the total thickness, $\varepsilon_{1,2}$ are the complex dielectric constants of the layers, and θ_B is the Bragg angle satisfying the condition

$$\mathrm{Re}[\varepsilon_1\gamma + \varepsilon_2(1 - \gamma)] - \sin^2 \theta_B = q^2/4k_0^2. \quad (2)$$

Equation (1) holds for the case in which the total thickness L is smaller than the characteristic absorption length l:

$$L < l = q\{4k_0^2 \, \mathrm{Im}[\varepsilon_1\gamma + \varepsilon_2(1 - \gamma)]\}^{-1}. \quad (3)$$

It follows from Eq. (1) that the angle-integrated reflection coefficient is independent of the thickness fluctuation ξ:

$$R^I = \int_{-\infty}^{+\infty} R(\theta)\mathrm{d}\theta = (k_0 \sin \pi\gamma)^2/ (2\pi^2 q \sin 2\theta_B)|\varepsilon_1 - \varepsilon_2|^2 \exp(-q^2\sigma^2)L. \quad (4)$$

The average size and the dispersion of the thickness fluctuations are determined by

$$\int_0^L \xi(x)\mathrm{d}x = [(2Ldk_0^2 \sin 2\theta_B)/(R^I q^2)](\partial P_i/\partial\delta|_{\delta=0}), \quad (5)$$

$$\int_0^L \xi(x)^2\mathrm{d}x = [(4Ld^2k_0^4 \sin^2 2\theta_B)/(R^I q^4)](\partial^2 P_r/\partial\delta^2|_{\delta=0}), \quad (6)$$

respectively, where $P_{i,r}$ is, respectively, the imaginary and the real part of the Fourier transform of the reflection coefficient:

$$P = \int_{-\infty}^{+\infty} R(\theta)\exp(i\theta\delta)\mathrm{d}\theta. \quad (7)$$

The ratio of the integrated reflection coefficients (4) at different wavelengths (for example, λ_1 and λ_2) is dependent only on the density and on the composition of the two layers forming the multilayer:

$$R^I(\lambda_1)/R^I(\lambda_2) = |[\varepsilon_1(\lambda_1) - \varepsilon_2(\lambda_1)]/[\varepsilon_1(\lambda_2) - \varepsilon_2(\lambda_2)]|^2[\sin 2\theta_B(\lambda_1)/\sin 2\theta_B(\lambda_2)]. \quad (8)$$

Furthermore, we assume layers A and B to be solid solutions with a mass concentration of component A in layer A of C_A. Obviously the mass concentration of the other component B in layer A is then $(1 - C_A)$. The dielectric susceptibility of material A in this case is of the form

$$\chi_A = r_e\lambda^2 N_A \rho_A [f_A C_A/A + f_B(1 - C_A)/B] \quad (9)$$

and similarly for material B; ρ is the density of the ith film, N_A is Avogadro's number, r_e is the classical electron radius, A, B and f_A, f_B are the atomic weights and the scattering factors of the materials, respectively. When the reflectance has been measured at four wavelengths, we can determine the density (ρ_A,

ρ_B) and the composition (C_A, C_B) of the layers by using Eq. (8) for four pairs of wavelengths. Then, using Eq. (1) or (4) for two different wavelengths, it is possible to find the roughness dispersion σ^2 and the thickness ratio γ for the two layers. The period is then determined from Eq. (2).

Equation (1) can be applied to superthin multilayers only, if the influence of the crystalline lattice discreteness on the reflectance is taken into account.[24] Indeed, in the context of a one-dimensional model for the crystal superlattice, we find for reflectance R

$$R = R_o R_d = R_o \left(\frac{\sin \pi a/d}{\pi a/d} \right)^2, \qquad (10)$$

where a is the parameter of the crystalline lattice, d is the period of the superlattice, R_o is the Fresnel reflectance of the multilayer in the Bragg maximum neglecting the crystal structure, obtained in the solidity approximation $a/d \to 0$, R_d is the scaling factor that accounts for the discreteness.

From Eq. (10) it follows that a relative error arising by utilization of the solidity approach becomes comparable with the experimental error of ~10%, when the superlattice period d is equal to approximately 8 times the lattice parameter a. This estimate clearly indicates that the discreteness of a crystalline superlattice should be accounted for with higher accuracy in determining the parameters of short-period nanolayers.

For example, the characteristics calculated for the Cr/Sc sample ($N = 185$, $d = 1.63$ nm) are as follows: $C_{Cr} = 0.94$, $C_{Sc} = 0.96$, $\rho_{Cr} = 6.57$ g/cm^2, $\rho_{Sc} = 3.65$ g/cm^2, $\gamma = 0.46$, $d_{Cr} = 0.75$ nm, $d_{Sc} = 0.88$ nm, $\sigma = 0.28$ nm. The sum $\Sigma\xi = 0.37$ nm of the deviations and the sum $\Sigma\xi^2 = 0.148$ nm^2 of the squared deviations were calculated in accordance with Eqs. (5) and (6). The parameters of all investigated multilayers, which were obtained according to this procedure, are given in Table 1.

3. Experimental

The Cr/Sc multilayers have been produced with magnetron sputtering. Eighteen different samples produced on standard Si (100) wafers ($\sigma \approx 0.4$ nm rms) and one sample sputtered on a thin (120 nm) Si_3N_4 membrane for use in transmission were investigated. The coating was performed under an Ar atmosphere of 0.05 Pa. The planar magnetrons had a diameter of 140 mm. Sc was coated by rf sputtering (13.56 MHz) with an incident power of 100–150 W. Cr was coated by dc magnetron sputtering with a power of 150 W. The deposition rates were between 0.05 and 0.1 nm/s. The substrates were mounted on a special table rotating over the targets at a height of 90 mm.

All multilayers were first characterized with monochromatic unpolarized soft-ray radiation emitted from an x-ray tube source at wavelengths of 4.47 nm (CK_α), 3.14 nm (TiL_β) 2.74 nm (TiL_α), 1.76 nm (FeL_α), 1.6 nm (CoL_α), 1.46 nm (NiL_α), 1.33 nm (CuL_α), 0.99 nm (MgK_α).[17]

Table 1. Relevant Parameters of all Investigated Cr/Sc Multilayers

Period d (nm)	Number of Layer Pairs P	Thickness Ratio $\gamma\, d_{Cr}/(d_{Cr} + d_{Sc})$
	Cr/Sc reflection multilayers	
3.14	150	0.55
2.55	150	0.49
2.35	100	0.5
2.32	100	0.5
2.30	200	0.42
2.24	82	0.5
2.14	250	0.49
2.04	200	0.49
1.80	250	0.53
1.76	200	0.58
1.73	235	0.45
1.66	250	0.45
1.63	185	0.46
1.60	250	0.49
1.59	200	0.5
1.59	300	0.5
1.57	250	0.66
1.55	250	0.5
	Cr/Sc transmission multilayer	
1.57	250	0.66

In Table 1 the relevant parameters of all the investigated Cr/Sc multilayers are listed.

We did the synchrotron radiation measurements described here by using the operational UHV-reflectometer chamber at the BESSY-beamline PM 4 in three beamtime shifts in 1996/1997.[25,26] The experimental arrangement is shown schematically in Fig. 3. The plane mirror/plane grating (1200-line/mm) combination of the SX700-type Petersen monochromator[27] (PM 4) delivers the dispersed synchrotron radiation onto the ellipsoidal mirror, which focuses light vertically onto the fixed exit slit with strong demagnification of the source. For reduction of higher orders the monochromator can be operated in the higher-order suppression mode by changing the incidence angles onto the mirror/grating combination (c factor; standard mode, $c = 2.25$). For transmission measurements c was set to 1.65. In the standard mode the higher-order contribution was measured to be between 10% and 25% in the range from 200 to 450 eV; at $c = 1.65$ it is less than 15%.[28] This, in combination with the increasing detector efficiency for higher energies, leads to an underestimate of the reflectance data between 1.1 and 1.6. The results in this article have, however, not been corrected with respect to higher orders. The linear polarization is estimated to be better than 90% in the energy range of interest.

For our measurements the BESSY triple-axis reflectometer/diffractometer was coupled to this beamline (Fig. 3). It is operated with all three motor-driven goniometers in vacuum and is used as a multipurpose instrument for optical characterization at any UV or soft-x-ray beamline. A differential pumping stage separates the 10^{-7}-mbar pressure of

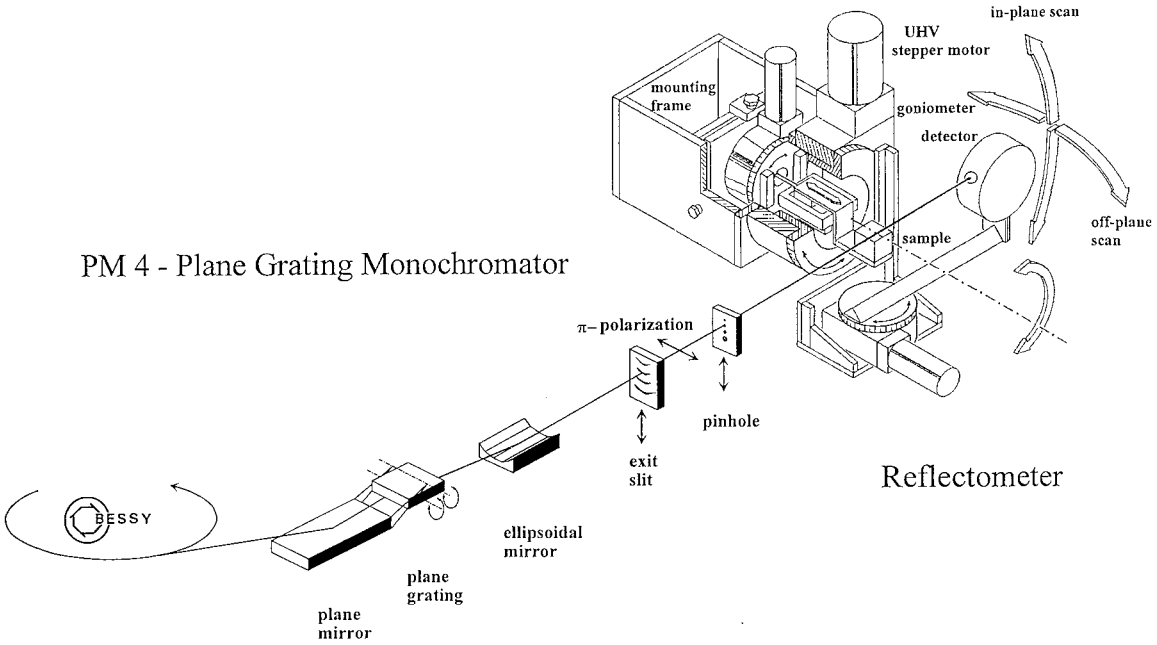

Fig. 3. Schematic drawing of the experimental setup at BESSY. The triple-axis UHV reflectometer/diffractometer is coupled to the exit slit of the bending magnet beamline PM 4 of the SX700 type.[25–27]

the reflectometer from the 10^{-9}-mbar pressure of the beamline. The reflectometer is equipped with entrance pinholes of various sizes between 0.14 and 2.5 mm, positioned behind the exit slit close to the position of the horizontal focus of the ellipsoidal mirror. The incident intensity is monitored during the measurements with Au or Cu meshes. For the intensity reflected from the sample and for the direct incident beam the same GaAsP diode[29] with a noise level of 30 fA is used.

For efficient data collection a new sample holder accepting up to three samples of any dimension to 150 mm × 50 mm × 50 mm was constructed. A three-dimensional scan option (Bragg scan) was implemented into the computer control that enables scanning simultaneously the incoming photon energy while scanning the multilayer around the Bragg peak ($h\nu$–θ–2θ scan). This feature is especially useful for investigations of near-edge absorption structures. Figure 4 shows the Bragg curves (θ–2θ scans) in the region of the Cr $2p_{3/2}$ and $p_{1/2}$ absorption edges, demonstrating the drastic changes in reflectance across these resonances.

4. Results

A. Reflection Multilayers

A variety of 19 samples of Cr/Sc multilayers with periods between 1.5 and 3.1 nm were investigated both with unpolarized light and with linearly polarized soft-x-ray synchrotron radiation at the design energies. As an example Fig. 5 shows the reflected intensity from a Cr/Sc multilayer fixed at 80° angle of incidence. The incoming photon energy was scanned, and the data were normalized to the incident intensity. At a d spacing of 2.24 nm the first Bragg peak (5% peak reflectance) appears close to the C 1s edge. The interference structure (Kiessig fringes) is clearly resolved, demonstrating the homogeneity of the individual layers. A fit with a REFLEC calculation yields a roughness parameter of σ = 0.3 nm.

A detailed investigation of the multilayer behavior

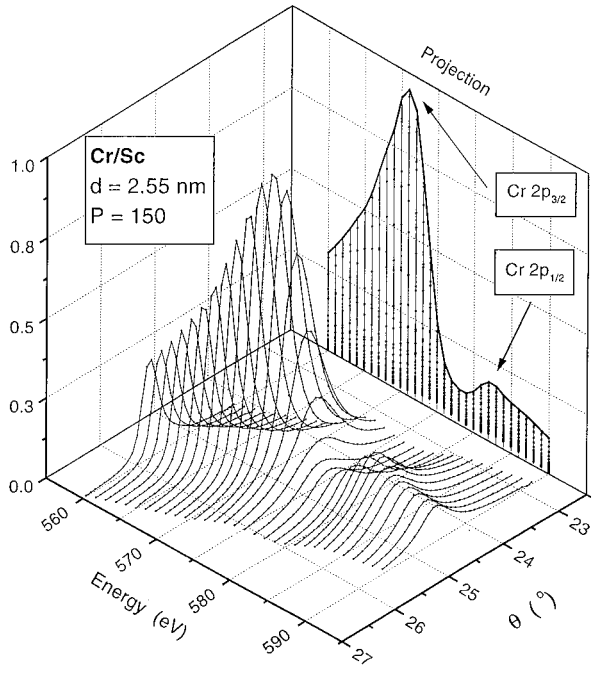

Fig. 4. Bragg scan ($h\nu$–θ–2θ) of a Cr/Sc multilayer around the Cr $2p_{3/2}$ and $p_{1/2}$ absorption edges. For each photon energy a θ–2θ scan around the Bragg peak was performed. The projection shows the peak reflectance data.

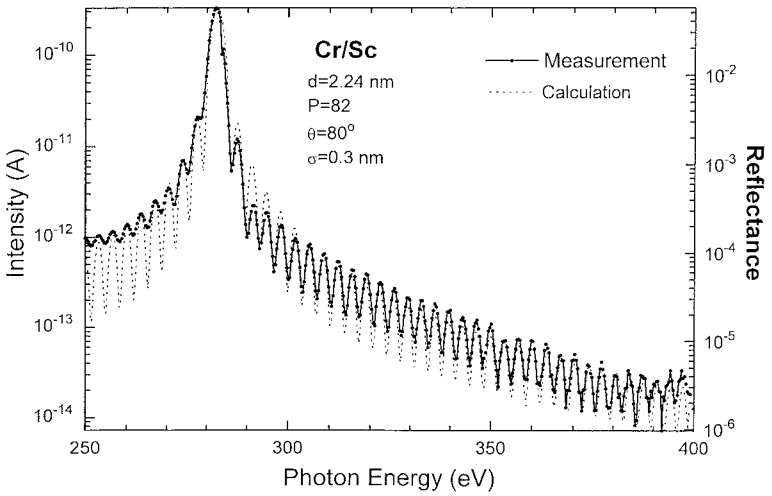

Fig. 5. Intensity reflected from a Cr/Sc multilayer as a function of photon energy at an incidence angle of $\theta = 80°$. Symbols with solid curve, experimental data. The fit (dotted curve) yields a roughness parameter of $\sigma = 0.3$ nm. The intensity is normalized with respect to the incident intensity.

near the Cr 2*p* edge is shown in Fig. 6. The top figure represents the peak reflectance obtained by scanning the photon energy through the resonance, with the multilayer kept on the Bragg maximum (see Fig. 4). The fine-structure splitting into $p_{3/2}$ and $p_{1/2}$, which the Henke table does not take into account (see Fig. 1), is clearly resolved. The corresponding energy spectra are shown in the lower part for four different angles of incidence θ_B. Note that,

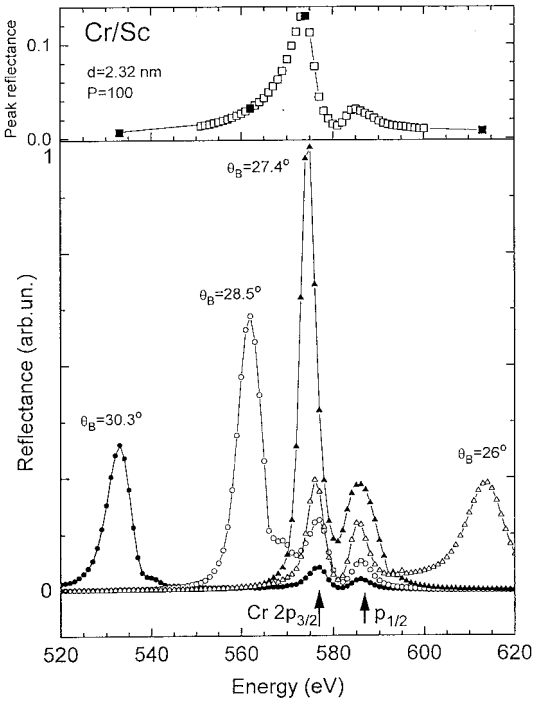

Fig. 6. Intensity reflected from a Cr/Sc multilayer as a function of the photon energy in the vicinity of the Cr 2*p* absorption edge for varies angles of incidence θ. Note that the resonant reflection peaks stay fixed at the $2p_{3/2}$ and $p_{1/2}$ edges, while the Bragg peak is moving through the resonance.

in addition to the Bragg-reflection peaks, two peaks at the Cr $2p_{3/2}$ and $2p_{1/2}$ absorption edges show up. In contrast to the Bragg peak, the energies at which these resonant reflection peaks appear are fixed at the resonance position and are independent of the angle. These resonant reflection peaks arise owing to atomic transitions between the occupied 2*p* and the empty 3*d* states. Their intensity is modulated by the Bragg-reflection peak: The intensities of both the resonant peaks and the Bragg peak are drastically enhanced when both peaks overlap. The increasing reflectance below the absorption edge (Fig. 6, top) can thus be explained by the combination of Bragg reflection and atomic resonance. The decreasing reflectance above the absorption edge is explained by the strong absorption. This interplay of both effects leads to a maximum Bragg reflection 2–3 eV below the edge. This common phenomenon has been observed also at the 2*p* edge of Sc and at other transition metals such as Ti and V.[21]

In Fig. 7 a selection of the peak reflectance data obtained for some of the investigated multilayers is depicted. These data were extracted from Bragg scans such as those shown in Fig. 4. All multilayers show a strong enhancement of the peak reflectance at the 2*p* absorption edges of Sc (left panel) and Cr (right panel) reaching very high values, to 18%. The incidence angle changes with energy according to the Bragg equation. The value at the lowest energy for each curve corresponds to normal incidence. Note that close to the Sc resonance a normal-incidence reflectance of 7% at 395 eV has been achieved for the multilayer with $d = 1.57$ nm, which was explicitly optimized for this edge. Thus for the time being this Cr/Sc multilayer is the best entry in the world wide web multilayer survey.[30]

All the multilayers perform equally well at both edges. Since the number of periods is the same for all multilayers, the dependence of the performance on

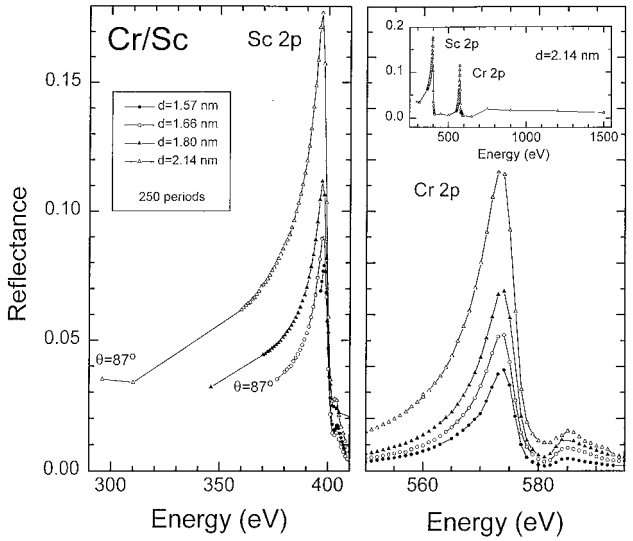

Fig. 7. Peak reflectance data for various Cr/Sc multilayers as a function of the photon energy for the Sc and the Cr 2*p* edges, extracted from Bragg scans such as shown in Fig. 4. The inset shows the reflectance in the total working range.

the period thickness is obvious from this figure. Fits to these four curves yield average interface-roughness values σ between 0.38 and 0.43 nm.

Corresponding to the resonance behavior of the peak reflectance, the energy resolution of the multilayers also changes throughout the resonance owing to the changing penetration depth of the light falling onto the multilayer. This is shown in Fig. 8 for selected Cr/Sc samples. Since the number of periods is the same for all multilayers, the resolution is mainly determined by the period spacing, i.e., the resolution increases with a decreasing period owing to the higher number of periods reached.

In Fig. 9 a summary of the peak reflectance data is shown for all the investigated multilayers, plotted as a function of their period d for two energies: for the peak position of the Sc (Fig. 9, top) and of the Cr resonance (Fig. 9, bottom). These data were extracted from the synchrotron radiation measurements (solid symbols), such as those shown in Fig. 7, and from measurements with unpolarized radiation from a laboratory x-ray source (open symbols). The incidence angle changes from normal to grazing incidence, as shown, and simultaneously the figure of merit ratio σ/d improves. Both effects add up to an improved performance with larger periods, as expected.

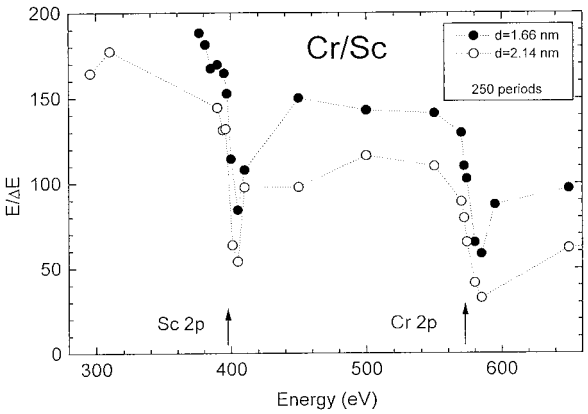

Fig. 8. Resolving power for selected Cr/Sc multilayers in the region of the Cr and Sc 2*p* edges. Data were calculated from the FWHM peak width of the θ–2θ curves.

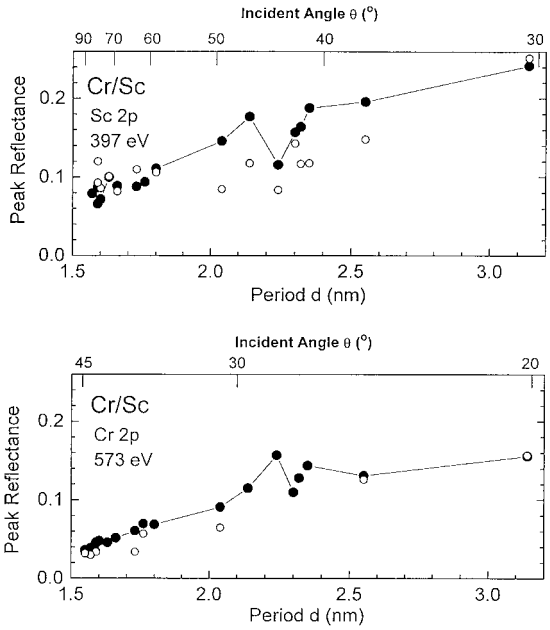

Fig. 9. Peak reflectance data as a function of the period (and the corresponding angle of incidence) for all investigated Cr/Sc multilayers for the energy of the Sc 2*p* (top) and of the Cr 2*p* edge (bottom). Solid symbols, results from synchrotron radiation measurements with linear polarized light; open symbols, results with unpolarized light from an x-ray tube at 395 and 574 eV.

The normal-incidence reflectance data are shown in Fig. 10, top, the data obtained for the 45° incidence angle in Fig. 10, bottom. The data are displayed as a function of the multilayer period and of the corresponding photon energy.

The data are influenced not only by the ratio σ/d but also by the anomalous dispersion around the Sc and Cr 2*p* resonances. Note that the optimum performance is obtained for the multilayer matched to the Sc edge (d = 1.57 nm) as shown in Fig. 7. For the next smallest multilayer (d = 1.55 nm) corresponding to a photon energy above the edge the performance is drastically reduced. This same multilayer, however, performs excellently at θ = 45°, since it is matched to the Cr edge at this angle. This experimentally determined reflection curve for normal incidence is thus equivalent to the calculated curves of Fig. 1. Moreover the roughness values can be directly deduced from the measured data. Upper and lower roughness limits are plotted as full curves.

A summary of the individual roughness values for all multilayers is given in Fig. 11. We obtained these data by fitting the reflectance curves measured

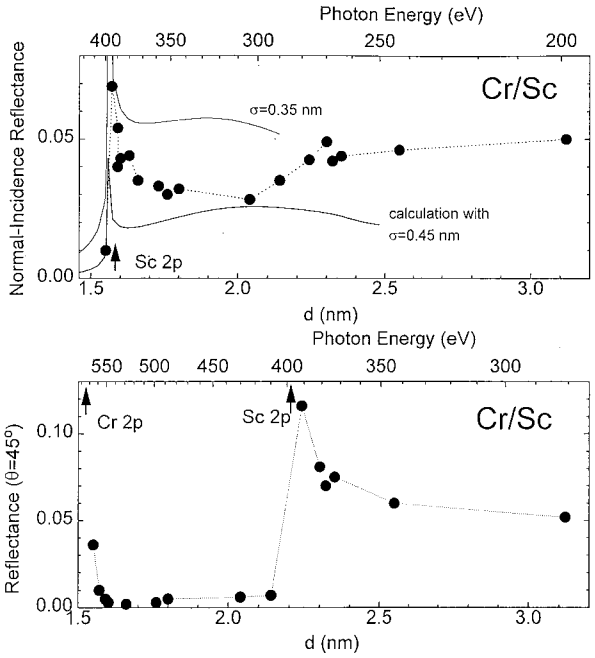

Fig. 10. Peak reflectance in normal incidence (top) and for an incidence angle of 45° (bottom) of Fig. 7 as a function of the period for all investigated Cr/Sc multilayers. Note the record value of 7% at 395 eV obtained with a period of 1.57 nm.

near the Cr 2*p* edge, using the Nevot–Croce model.[31] This model is a modified Debye–Waller approach that takes into account individual roughnesses for the substrate and both materials at every boundary on the basis of the complex amplitudes. However, only one integral roughness value for each material was taken throughout the multilayer stack. The best agreement to experiment was obtained by assuming equal roughnesses for both materials. Since all the multilayers have been fitted in the same way, the following trends can be extracted from the data:

(1) The roughness tends to increase slightly with the number of periods. This may indicate unsufficient stabilization of sputter parameters during the (up to 2 h of) growth of the multilayers.

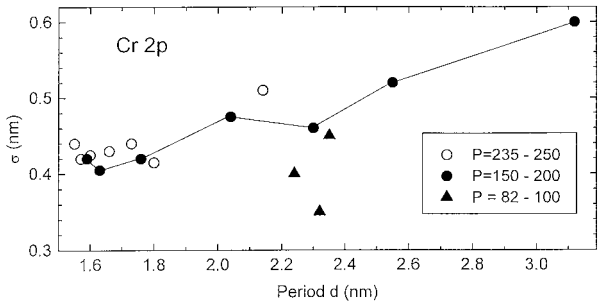

Fig. 11. Roughness values extracted from the reflectance data of Fig. 7 for all Cr/Sc multilayers. The fit to the experimental data was done in the region of the Cr 2*p* edge. The roughness data apply to both materials. Substrate roughness is 0.4 nm.

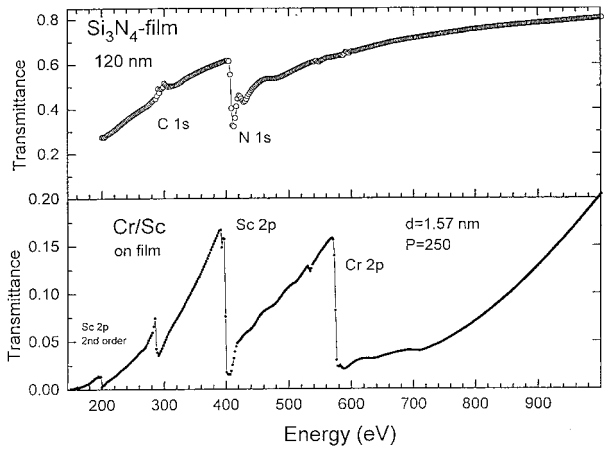

Fig. 12. Normal-incidence transmission of a Si_3N_4 film without (top) and with (bottom) a Cr/Sc multilayer in the soft-x-ray range.

(2) The lower limit of the roughness is mainly determined by the substrate roughness of ~0.4 nm. Further improvement of the substrates seems therefore to be necessary.

(3) A systematic trend of a decreasing roughness with decreasing period is observed. This peculiarity was discussed in Ref. 32 and is, for this material combination, most likely a real effect caused by partial crystallization of the layers, already observed in W/Sb structures.[12,14] On the one hand, it may also be an indication of the limits of the roughness model for these superthin multilayer structures investigated. For example, for the sample with $d = 1.57$ nm the individual Sc layer thickness is only 0.53 nm, whereas the calculated roughness of 0.4 nm is more than half of the layer thickness. On the other hand, the density of the layers is very likely away from the bulk density values used in the fitting procedure. In addition, the optical constants of the sputtered layers may differ significantly from the Henke-data values used in the calculation, especially in the region of absorption edges.[33]

Therefore the data shown allow for a systematic comparison of all investigated multilayers rather than to be interpreted rigorously as absolute rms roughnesses. For more detailed information about the real physical composition of the multilayer stack, more refined fitting procedures, taking into account the problem of the correlation of roughness, their spatial frequencies, the individual layer thicknesses, densities, and optical constants, would be necessary.

B. Transmission Multilayers

The transmission multilayers to be used as phase-retarding elements in our polarimeter are grown on 120-nm thin Si_3N_4 films etched chemically from a Si wafer (15 mm × 15 mm) in a 3 mm × 5 mm window area. According to Fig. 12 (top) the support structure is highly transparent in the water window except for the dominant absorption feature around the N 1*s* edge at 400 eV. As expected, the transmission

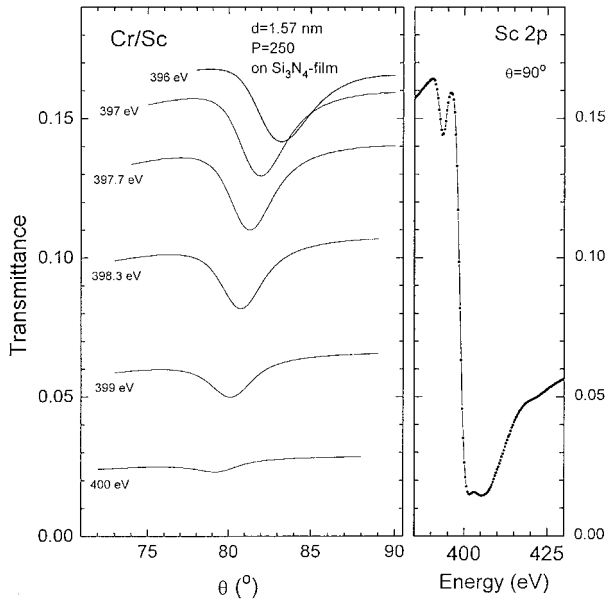

Fig. 13. Dependence of the transmission of the Cr/Sc-multilayer/membrane structure on the angle of incidence at various energies close to the 2*p* edge of Sc (left panel). The transmission exhibits a pronounced Bragg minimum within the absorption edge corresponding to the Bragg maximum in reflection geometry. The energy-dependent transmission curve (right panel) is taken from Fig. 12. Note the experimentally resolved spin-orbit splitting of the edge into $2p_{3/2}$ and $2p_{1/2}$.

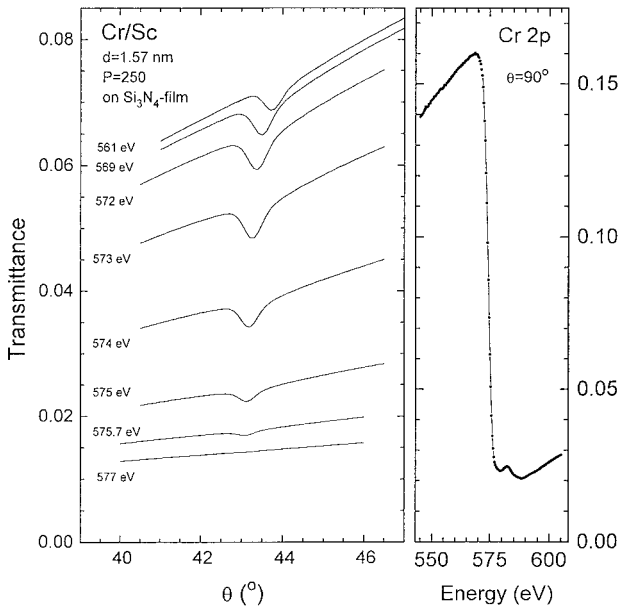

Fig. 14. Dependence of the transmission of the Cr/Sc-multilayer/membrane structure on the angle of incidence at various energies close to the 2*p* edge of Cr (left panel). The transmission exhibits a pronounced Bragg minimum within the absorption edge corresponding to the Bragg maximum in reflection geometry. The energy-dependent transmission curve (right panel) is taken from Fig. 12. Note the experimentally detected spin-orbit splitting of the edge into $2p_{3/2}$ and $2p_{1/2}$.

of the multilayer structure shows strong absorption at the corresponding Cr and Sc 2*p* edges, of which the latter coincides with the N 1*s*-edge absorption of the membrane. In addition the Cr and Sc absorption in second order around 200 eV and 287 eV, respectively, can be identified.

Measurements of the angular dependence of the transmitted intensity are shown in Figs. 13 and 14 for the Sc and Cr 2*p* edges, respectively. The data show the well-pronounced transmission minima at photon energies close to the absorption edges of the respective materials. These minima correspond to the Bragg maxima in reflection geometry. This is encouraging since, as shown previously,[4,34] this minimum, which appears only in *s*-polarization geometry, is an indication of phase-shifting properties, which, however, cannot experimentally be determined with reflectometry.

5. Conclusions

We have presented a systematic investigation of sputter-deposited ultrathin Cr/Sc multilayers, using tunable synchrotron radiation in the soft-x-ray range. The period spacing varied in the range between 1.5 and 3.1 nm, which determines that the working range is in the soft-x-ray range with special emphasis on the water window. An excellent performance was measured close to the 2*p*-absorption edges of Cr (574 eV) and Sc (399 eV), where the reflectance and the energy resolution are resonantly enhanced. A value of 7% for the normal-incidence reflectance at 395 eV was measured for a multilayer with a period of $d = 1.57$ nm, matched to the resonance energy. This is the highest value measured so far at this energy.

Note that in this study only Cr/Sc multilayers have been examined. Many other material combinations with a high theoretical potential still must be investigated. Work is in progress for systematic studies on other promising multilayer candidates for certain energy ranges where Sb (460–530 eV), Ti (410–450 eV), and C (190–280 eV) are used as spacer materials and W, Ni, Co, Fe, and Cr as absorbers.

This research is supported by the European Community (contract ERBFMGECT950007). The multilayers were produced within the framework of the programs Synchrotron Radiation and Solid State Nanostructures supported by the Ministry of Science and Technical Politics of Russia.

We are indebted to M. Mertin of the BESSY optics group for kind assistance during the beam time. We thank Leonid Shmaenok of the FOM Institute for Plasma Physics, Rijnhuizen, Nieuwegein, The Netherlands, for successfully transporting the delicate multilayer membranes to and from Nizhny Novgorod.

References and Notes

1. E. Spiller, *Soft-X-Ray Optics* (SPIE Optical Engineering Press, Bellingham, Wash., 1994).
2. F. Schäfers, M. Grioni, J. Wood, H. van Brug, E. J. Puik, M. Dapor, and F. Marchetti, "Application of W/Si multilayers for monochromatization of soft-x-ray synchrotron radiation," in *X-Ray Multilayers for Diffractometers, Monochromators, and*

Spectrometers, F. E. Christensen, ed., Proc. SPIE **984,** 23–30 (1988).
3. J. Kortright, H. Kimura, V. Nikitin, K. Mayama, M. Yamamoto, and M. Yanagihara, "Soft-x-ray (97-eV) phase retardation using transmission multilayers," Appl. Phys. Lett. **60,** 2963–2965 (1992).
4. S. DiFonzo, W. Jark, F. Schäfers, H. Petersen, A. Gaupp, and J. Underwood, "Phase-retardation and full polarization analysis of soft-x-ray synchrotron radiation close to the carbon *K* edge by use of a multilayer transmission filter," Appl. Opt. **33,** 2624–2632 (1994).
5. S. DiFonzo, B. R. Müller, W. Jark, A. Gaupp, F. Schäfers, and J. H. Underwood, "Multilayer transmission phase shifters for the carbon K edge and the water window," Rev. Sci. Instrum. **66,** 1513–1516 (1995).
6. J. Viefhaus, L. Avaldi, G. Snell, M. Wiedenhöft, R. Hentges, A. Rüdel, F. Schäfers, D. Menke, U. Heinzmann, A. Engelns, J. Berakdar, H. Klar, and U. Becker, "Experimental evidence for circular dichroism in the double photoionization of helium," Phys. Rev. Lett. **77,** 3975–3978 (1996).
7. N. N. Salashchenko, Yu. Ya. Platonov, and S. Yu. Zuev, "Multilayer x-ray optics for synchrotron radiation," Nucl. Instrum. Methods A **359,** 114–120 (1995).
8. S. V. Bobashev, A. V. Golubev, Yu. Ya. Platonov, L. A. Shmaenok, G. S. Volkov, N. N. Salashchenko, and V. I. Zayzev, "Absolute photometry of pulsed fluxes of ultrasoft x-ray radiation," Phys. Scr. **43,** 356–367 (1991).
9. J. Kirz, C. Jacobsen, and M. Howells, "Soft x-ray microscopes and their biological applications," Q. Rev. Biophys. **28,** 33–130 (1995).
10. E. Spiller, T. W. Barbee, L. Golub, K. Kalata, G. Nystrom, and A. Viola, "Results from the recent flight of the IBM/SAO x-ray telescopes," in *Multilayer and Grazing Incidence X-Ray/EUV Optics II*, R. B. Hoover and A. B. Walker, eds., Proc. SPIE **2011,** 391–401 (1993).
11. A. D. Akhsakhalyan, N. N. Kolachevsky, M. M. Mitropolsky, E. N. Ragozin, N. N. Salashchenko, and V. A. Slemzin, "Fabrication and investigation of imaging normal-incidence multilayer mirrors with a narrow-band reflection in the range λ = 4.5 nm," Phys. Scr. **48,** 566–570 (1993).
12. N. N. Salashchenko, S. V. Gaponov, A. D. Akhsakhalyan, S. S. Andreev, Yu. Ya. Platonov, N. I. Polushkin, E. A. Shamov, S. I. Shinkarev, and S. Yu. Zuev, "Normal incidence imaging multilayer x-ray mirrors with periods of nanometer and subnanometer scale," in *Multilayer and Grazing Incidence X-Ray/EUV Optics II*, R. B. Hoover and A. B. Walker, eds., Proc. SPIE **2011,** 402–412 (1993).
13. I. V. Kozhevnikov, A. I. Fedorenko, V. V. Kondratenko, Y. P. Pershin, S. A. Yulin, E. N. Zubarev, H. A. Padmore, K. C. Cheung, G. E. van Dorssen, M. Roper, L. L. Balakireva, R. V. Serov, and A. V. Vinogradov, "Synthesis and measurement of normal-incidence x-ray multilayer mirrors optimized for a photon energy of 390 eV," Nucl. Instrum. Methods A **345,** 594–603 (1994).
14. S. S. Andreev, M. Müller, Yu. Ya. Platonov, N. I. Polushkin, N. N. Salashchenko, F. Schäfers, S. I. Shinkarev, D. M. Simanovsky, and S. Yu. Zuev, "Small *d*-spacing multilayer structures for the photon energy range $E > 0.3$ keV," in *Superintense Laser Fields: Generation, Interaction with Matter, and X-Ray Sources*, S. V. Gaponov and V. M. Gordienko, eds., Proc. SPIE **1800,** 195–208 (1991).
15. F. E. Christensen, S. Zhu, A. Hornstrup, H. W. Schnopper, P. Plag, and J. Wood, "X-ray study of state-of-the-art small *d*-spacing W/B_4C multilayers," J. X-ray Sci. Technol. **3,** 1–13 (1991).
16. L. A. Shmaenok, Yu. Ya. Platonov, N. N. Salashchenko, A. A. Sorokin, D. M. Simanovskii, A. V. Golubev, V. P. Belik, S. V. Bobashev, F. Bijkerk, E. Louis, F. G. Meijer, B. Etlicher, and A. Y. Grudsky, "Multilayer EUV/x-ray polychromators for plasma diagnostics," J. Electron Spectrosc. Related Phenom. **80,** 259–262 (1996).
17. N. N. Salashchenko, Yu. Ya. Platonov, and S. Yu. Zuev, "Multilayer optics for soft x rays," Phys. Chem. Mech. Surf. **11**(10), 1017–1034 (1995).
18. H.-Ch. Mertins, F. Schäfers, A. Gaupp, F. Schmolla, W. Gudat, S. Di Fonzo, G. Soullie, W. Jark, R. Walker, M. Ericksson, and R. Nyholm, "A detector for circularly polarized soft-x-ray radiation," in *Book of Abstracts*, *Workshop on Nanometer-Scale Methods in X-Ray Technology* (*NSMXT*), Lisbon, 6–9 October 1997.
19. B. L. Henke, E. M. Gullikson, and J. C. Davis, "X-ray interactions: photoabsorption, scattering, transmission and reflection at E = 50–30.000 eV, Z = 1–92," At. Data Nucl. Data Tables **54,** 181–342 (1993).
20. F. Schäfers and M. Krumrey, "REFLEC—A program to calculate soft-x-ray optical elements and synchrotron radiation beamlines," Tech. Ber. BESSY TB **201,** 1–17 (1996), BESSY GmbH, Lentzeallee 100, D-14195 Berlin.
21. H.-Ch. Mertins, F. Schäfers, H. Grimmer, D. Clemens, P. Böni, and M. Horrisberger, "W/C, W/Ti, Ni/Ti and Ni/V multilayers for the soft-x-ray range: experimental investigation with synchrotron radiation," to be published in Appl. Opt.
22. M. Yamamoto and T. Namioka, "Layer by layer design method for soft-x-ray multilayers," Appl. Opt. **31,** 1622–1630 (1992).
23. A. D. Akhsakhalyan, A. A. Fraerman, N. I. Polushkin, Yu. Ya. Platonov, and N. N. Salashchenko, "Determination of layered synthetic microstructure parameters," Thin Solid Films **203,** 317–326 (1991).
24. S. L. Duan and J. O. Artman, "Study of the growth characteristics of sputtered Cr thin films," J. Appl. Phys. **67,** 4913–4915 (1990).
25. W. Jark and J. Stöhr, "A high-vacuum triple-axis diffractometer for soft-x-ray scattering experiments," Nucl. Instrum. Methods A **266,** 654–658 (1988).
26. C. Jung, ed., *Research at BESSY, A User's Handbook* (BESSY, Berlin, Germany, 1995).
27. H. Petersen, C. Jung, C. Hellwig, W. B. Peatman, and W. Gudat, "Review of plane grating focusing for soft-x-ray monochromators," Rev. Sci. Instrum. **66,** 1–14 (1995).
28. U. Flechsig, F. Eggenstein, R. Follath, and F. Senf, "Diffraction efficiency and high order suppression of gratings for synchrotron radiation," in *Gratings and Grating Monochromators for Synchrotron Radiation*, W. R. McKinney and C. A. Palmer, eds., Proc. SPIE **3150,** 9–17 (1997).
29. M. Krumrey, E. Tegeler, J. Barth, M. Krisch, F. Schäfers, and R. Wolf, "Schottky type photodiodes as detectors in the VUV and soft-x-ray range," Appl. Opt. **27,** 4336–4341 (1988).
30. For further information on the multilayer survey, see http://www-cxro.lbl.gov/multilayer/survey.html.
31. L. Nevot and P. Croce, "Caracterisation des surfaces par reflexion rasante de rayons X. Application a l'etude du polissage de quelques verres silicates," Rev. Phys. Appl. **15,** 761–779 (1980).
32. J. B. Kortright, "Status and limitations of multilayer x-ray interference structures," J. Magn. Magn. Mat. **156,** 271–275 (1996).
33. R. Souflie and E. M. Gullickson, "Reflectance measurements on clean surfaces for the determination of optical constants of silicon in the extreme ultraviolet-soft-x-ray region," Appl. Opt. **36,** 5499–5507 (1997).
34. F. Schäfers, A. Furuzawa, K. Yamashita, M. Watanabe, and J. Underwood, "Beamsplitting and polarizing properties of Cr/C transmission multilayers close to the carbon *K*-edge," in *Physics of X-Ray Multilayer Structures*, Vol. 6 of 1994 Technical Digest Series (Optical Society of America, Washington, D.C., 1994), pp. 155–158.